Design and Synthesis of a Geopolymer-Enhanced Quasi-Crystalline Composite for Resisting Wear and Corrosion

M. Fevzi Ozaydin
Department of Mechanical Engineering,
Texas A&M University,
College Station, TX 77843

Hong Liang[1]
Department of Mechanical Engineering,
Texas A&M University,
College Station, TX 77843
e-mail: hliang@tamu.edu

Multiphase composites are attractive for improved mechanical performance and corrosion resistance. In this research, a new composite consisting quasi-crystalline $Al_{75}Mn_{14}Si_7Fe_4$ alloy of icosahedral, cubic α-AlMnSiFe, monoclinic $Al_{13}Fe_4$ phases, and ferro-silico-aluminate geopolymer was synthesized using rapid solidification and thermal treatment methods. The concentration of icosahedral phase (i-phase) was controlled and the formation of geopolymer was obtained through heat treatment. Characterization showed that the microhardness and wear resistance were increased with the amount of i-phase. The corrosion resistance, on the other hand, was improved with the existence of the geopolymer. This research demonstrates an effective approach in processing a multiphase composite that has desired properties and performance through multiphase design and composition. [DOI: 10.1115/1.4031400]

Keywords: quasi-crystals, icosahedral, geopolymer, friction and wear, corrosion resistance

1 Introduction

Since the discovery of icosahedral phase in rapidly solidified Al–Mn alloys [1,2], there have been great interests to develop alternative material systems [3–12]. The formation of icosahedral phase in Al_6Mn alloy was reported by Shechtman et al. in 1984 during rapid solidification via nucleation and subsequent crystal growth [1]. In following 30 year, this class of materials has attracted intense interests [13–17]. However, synthesis and characterization of AlMnSiFe-quasi-crystalline-based composites have yet to be achieved. There are some reports on quasi-crystal–polymer composite systems based on AlCuFe alloys. Mihoc et al. [18] and Anderson et al. [19] synthesized and characterized AlCuFe quasi-crystal alloy reinforced with ultrahigh molecular weight polyethylene (UHMWPE) for biomedical applications. Mechanical and surface properties of Al–Cu–Fe quasi-crystal with epoxy filler were reported by Bloom et al. [20–23]. In addition, Liu et al. studied the mechanical and tribological properties of AlCuFe quasi-crystal reinforced with polyamid 12 polymeric material [24]. Corrosion behavior of Al–Cu–Fe alloy containing quasi-crystalline phase was reported by Huttunen-Saarivirta and Tiainen [25]. Apart from AlCuFe quasi-crystal/polymer composite systems, Wang et al. alternatively synthesized and characterized Ti-based, Ti–Zr–Ni quasi-crystalline material doped with polyamid 12 fillers [26]. Table 1 shows some of the Al-based quasi-crystalline/polymer composites and their studied major properties below.

The unique combination of characteristics and properties has enabled geopolymers for various engineering applications. These properties stem from several beneficial features, such as good mechanical properties, excellent bonding with the matrix, and resistance to corrosive environments [27,28]. Geopolymers are considered as a special class of inorganic polymers which exist in both crystalline and noncrystalline structures. They can be synthesized through a chemical reaction involving alkali aluminosilicate oxides and aqueous alkali hydroxide yielding polymeric Si–O–Al bonds [29–32]. Crystalline form of geopolymers can be formulated in the form of M_n–(–Si–O–Al–O–)$_n$, where *M* being a cation such as iron, sodium, potassium, calcium, and "*n*" defining the degree of polycondensation [33,34]. Chemical components and the properties of geopolymers are shown in Table 2.

The addition of reinforcements into quasi-crystalline matrix is an alternative approach in designing new composites with desired properties [37,38]. In this study, we report the tribology and the corrosion behavior of $Al_{75}Mn_{14}Si_7Fe_4$ quasi-crystalline alloy matrix composite. This composite contains a ferro-silico-aluminate-geopolymer phase induced through annealing at elevated temperature for the first time. The mechanical properties as well as wear and corrosion performance will be investigated.

2 Experimental Details

2.1 Materials and Sample Preparation. The $Al_{75}Mn_{14}Si_7Fe_4$ alloy was prepared by melting and casting in a conventional vacuum arc furnace. High-purity commercial elements 99.99% Al (EM Science, Cherry Hill, NJ), 99.98% Fe (Sigma-Aldrich, St. Louis, MO), 99.9999% Si (ESPI Metals, Ashland, OR), and 99.9% Mn (Alfa Aesar, Ward Hill, MA) were used for this study. Ingots of 10 g were melted as an initial material. Each ingot was arc-melted four times under an argon atmosphere to obtain homogeneous structure and to prevent oxidation.

The $Al_{75}Mn_{14}Si_7Fe_4$ alloy samples were prepared as-cast and annealed conditions. Annealing was done using a Cress electric furnace at 300 °C for 30 hrs. The purpose and condition of

Table 1 Composition and properties of major quasi-crystalline/geopolymer composites

Composition	Major properties	References
$Al_{65}Cu_{23}Fe_{12}$-Epoxy	Wear	[6]
$Al_{65}Cu_{23}Fe_{12}$-UHMWPE	Wear/mechanical	[5]
$Al_{65}Cu_{23}Fe_{12}$-PA_{12}	Wear/mechanical	[8]
$Ti_{40.83}Zr_{40.83}Ni_{18.34}$	Wear	[9]

[1]Corresponding author.

Contributed by the Tribology Division of ASME for publication in the JOURNAL OF TRIBOLOGY. Manuscript received April 1, 2015; final manuscript received July 22, 2015; published online October 15, 2015. Assoc. Editor: Dae-Eun Kim.

Table 2 The comparison of composition and properties of geopolymers

	Aluminosilicate	SiO_2	Al_2O_3	CaO	MgO	K_2O	Vickers hardness (MPa)	Compressive strength (MPa)	References
Geopolymer	Metakaolin	64 ± 2	10 ± 1	19 ± 2	0–1	8 ± 1	191–242	28.7–70.4	[35,36]
	Calcined clay	58 ± 2	6 ± 1	25 ± 2	3 ± 0.5	9 ± 2	290–308	11–40	[35,36]

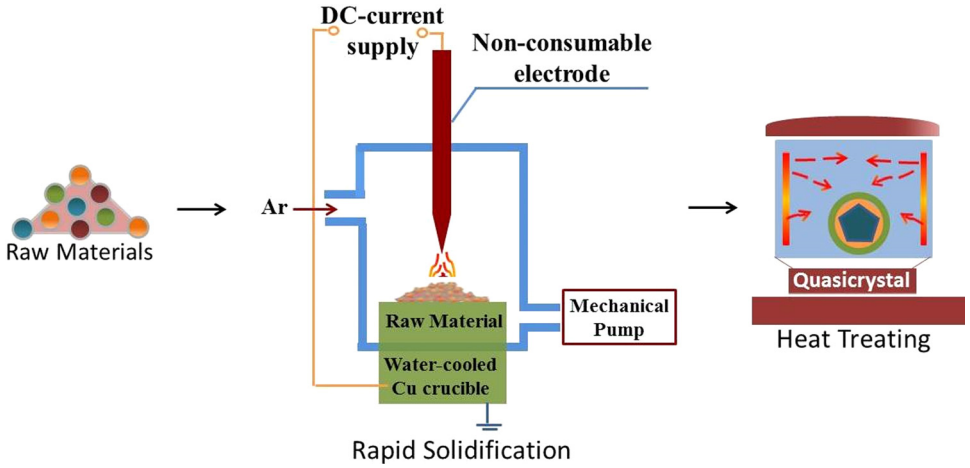

Fig. 1 Quasi-crystalline alloy process steps

annealing were to create oxides and the resulting geopolymers are yet to not sacrifice the mechanical properties induced by quasi-crystalline phase. Figure 1 shows the processing steps outlined in each sections.

Geopolymer samples were prepared in K32 chemical composition. The K32 represents the potassium silicate solution and the ratio of Si/Al to $H_2O/(Al_2O_3 + SiO_2)$, respectively. These samples are used as reference.

Samples were then mounted on a Buehler SimpliMet mounting press under 4.2 ksi pressure. Mounted specimens were grinded and autopolished using a Buehler ECOMet 250 grinder and polisher. Silicon carbide base polishing pads were used from 400 to 1200 grit followed by a final polishing using 0.5 μm alumina solution.

2.2 Characterization. Optical microscopic images were obtained using KEYENCE VHX-Z35 digital microscope. Laser confocal microscopy was done using KEYENCE VK-9710 violet color three-dimensional (3D) laser microscope.

X-ray diffraction (XRD) analysis was conducted to identify the phase structure of $Al_{75}Mn_{14}Si_7Fe_4$ alloy samples in both as-cast and annealed conditions. The samples were placed in the sample holder of a two-circle goniometer, enclosed in a radiation safety enclosure. The X-ray source was a 2.2 kW Cu X-ray tube, maintained at an operating current of 40 kV and 40 mA. The X-ray optics were the standard Bragg–Brentano parafocusing mode with the X-ray diverging from a divergence-limiting slit (1 mm) at the tube to strike the sample and then converging at a position sensitive X-ray detector (Lynx-Eye, Bruker-AXS). The two-circle 250-mm diameter goniometer was computer controlled with independent stepper motors and optical encoders for the θ and 2θ circles with the smallest angular stepsize of 0.0001 deg 2θ. The software suit for data collection and evaluation is windows based. Data collection is automated COMMANDER program by employing a data query language file. Data are analyzed by the program EVA.

Microhardness was measured using Hystiron model TS 75 triboscope nanoindenter. In order to assess the validity of wear and corrosion resistance of quasi-crystalline samples, tribological testing and potentiodynamic polarization experiments were conducted. Wear tests were carried out at room temperature using tribometer (CSM Instruments; Anton Paar Tritec SA, Peseux, Switzerland) with pin-on-disk configuration. The disks were made out of the material to be tested and the counter bodies were martensitic stainless steel balls with a diameter of 6 mm. A normal load of 2 N and constant sliding velocity of 0.3 m s^{-1} were applied. The total sliding distance was 0.5 km.

Corrosion data were acquired using an electrostate (Gamry Instruments, Warminster, PA) electrochemical measurement system. The working electrodes were ground, polished, and polarized in 0.1 M saline NaCl solution. The electrolytic cell consisted of working electrode, platinum counter electrode, and an Ag/AgCl reference electrode containing 3 M KCl as an electrolyte in Pyrex beaker. The polarization response was measured between −2000 and 2000 mV. The polarization rate was 50 mV s^{-1}.

3 Results and Discussion

3.1 Microstructural Characterization of As-Cast and Annealed Alloys. Figure 2(*a*) shows the XRD patterns of both as-cast and annealed alloys. The XRD spectrum of as-cast $Al_{75}Mn_{14}Si_7Fe_4$ alloy indicates the presence of quasi-crystalline phase (*i*-phase) along with a minor, cubic, α-AlMnSiFe phase. There is also an indication of a crystalline trace phase, $Al_{13}Fe_4$ consisting of a monoclinic crystal lattice. The XRD pattern of annealed sample shows a ferro-silico-aluminate (Fe–Al–Si–O), i.e., a geopolymer phase. It can also be seen clearly that XRD peaks mainly constituted of major quasi-crystalline phase (*i*-phase) and cubic α-AlMnSiFe. Quasi-crystalline phase (*i*-phase) and coexisting phases are metastable; therefore during annealing at 300 °C, the sample undergoes phase transformation. During sample preparation, in order to form a quasi-crystal–geopolymer hybrid system, the $Al_{75}Mn_{14}Si_7Fe_4$ alloy needs to be heated to a temperature sufficient enough to allow the transformation. During this process, a small amount peak shift was observed in some minor phases indicating transformation of those crystalline phases.

Scanning electron microscope (SEM) images of both as-cast and annealed structures of the $Al_{75}Mn_{14}Si_7Fe_4$ alloy were shown in Figs. 2(*b*) and 2(*c*). Both micrographs reveal the presence of phases formed during rapid solidification. $Al_{75}Mn_{14}Si_7Fe_4$ alloy is an icosahedral quasi-crystalline alloy which has been studied for phase identification previously [14]. $Al_{75}Mn_{14}Si_7Fe_4$ has a two-phase quasi-crystalline alloy one of which is the *i*-phase (icosahedra phase) being the main phase and the second of which is

the α-AlMnSiFe (cubic) being the minor phase. The unique five-fold crystal structure is easily identifiable. The relative amount of each phase was evaluated using IMAGEJ analysis. Results showed that the volume fraction of *i*-phase was at 70% in as-cast and was decreased to about 60% after thermal treatment. Based on the SEM images in Figs. 2(*b*) and 2(*c*), it can be seen in both figures that the quasi-crystalline phase (*i*-phase) is the dominant which appears in light color. In accordance with the XRD data, the annealed micrograph shows the decrease in quasi-crystalline *i*-phase and increase in cubic α-AlMnSiFe.

3.2 Mechanical Properties. Microhardness of the as-cast, arc-melted, and the geopolymer samples were determined in comparison with Aluminum 6061 alloy [39,40]. This alloy is one of the mostly used metals that its properties are standardized. The results are shown in Fig. 3. As-cast specimen had slightly higher values of hardness. This is in agreement with the XRD results discussed here. As the materials are annealed at 300 °C for 30 hrs, the amount of quasi-crystalline *i*-phase decreased and cubic α-AlMnSiFe phase increased while the hardness remains about the same value. This is desirable since we aimed to increase corrosion resistance without sacrifice hardness.

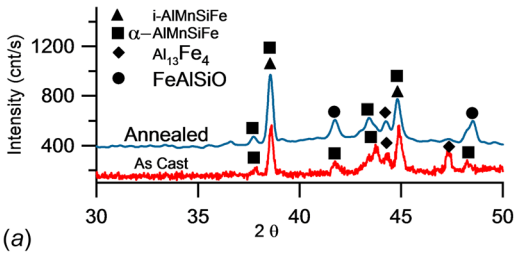

(*a*)

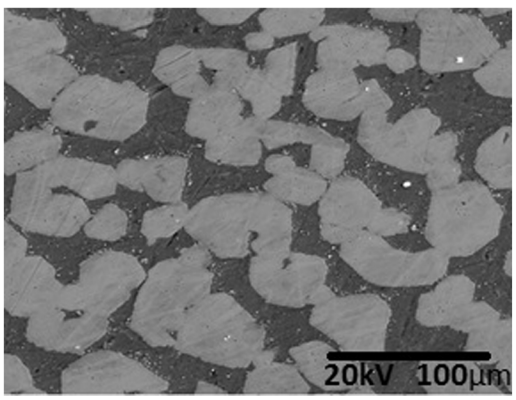

(*b*)

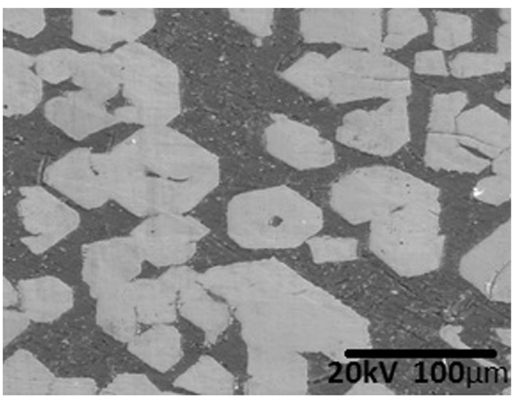

(*c*)

Fig. 2 (*a*) XRD patterns of $Al_{75}Mn_{14}Si_7Fe_4$ alloy and (*b*) and (*c*) SEM images showing the microstructure of as-cast and annealed conditions, respectively

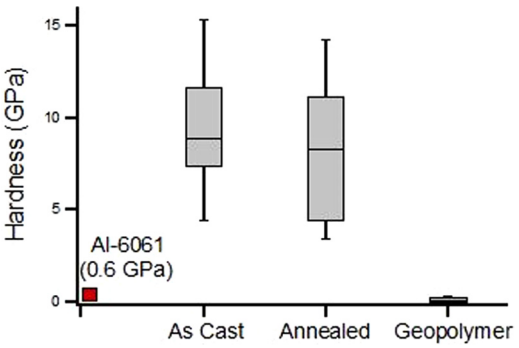

Fig. 3 Comparison of the microhardness data

3.3 Wear Resistance. Wear tests were conducted at room temperature using a tribometer with pin-on-disk configuration in a linear mode. The coefficient of friction data was obtained for three separate conditions against time and shown in Fig. 4. The coefficient of friction for the annealed sample was slightly higher than the as-cast specimen in the amount of 9%. This can be attributed to the decrease in hardness by the reduced amount of quasi-crystalline phase (*i*-phase) from as-cast to annealed condition. The high coefficient of friction of geopolymeric material could be due to the soft nature of polymers that deform under stress. The more contact area disperses more mechanical energy through contact. This is evidenced by the micrograph of the worn surface of the polymer as shown in Fig. 5(*i*), where the wear track is uniformly deformed.

As-cast and the annealed specimens both had similar wear behavior, both worn surfaces reveal abrasive wear rather than adhesive as seen in Figs. 5(*a*) and 5(*e*). The laser confocal microscopy was performed for both as-cast and annealed conditions, and the wear depths and wear volumes were calculated. As-cast sample shown in Figs. 5(*b*) and 5(*d*) had a wear volume of 0.55 mm^3 as compared to a value of 0.95 mm^3 in annealed sample shown in Figs. 5(*f*) and 5(*h*). The slight reduction in wear of annealed sample could be due to the decrease of the quasi-crystalline icosahedral phase as evidenced in Fig. 2(*a*). Since our main objective is to increase both hardness and corrosion resistance, the slight reduction in wear resistance is not significant if the corrosion resistance is increased. This will be discussed in Sec. 3.4.

The surface roughness was measured on both as-cast and annealed conditions. The average roughness, R_a, and root mean square roughness, R_q, values were obtained. The R_a and R_q values for as-cast and annealed $Al_{75}Mn_{14}Si_7Fe_4$ quasi-crystalline alloy are 0.793 μm, 1.039 μm and 0.890 μm, 1.248 μm, respectively. Data show that the roughness values increase due to annealing. It is believed that the phase transformation resulted in slight coarsening. The coefficient of friction during running period reflects the slight difference.

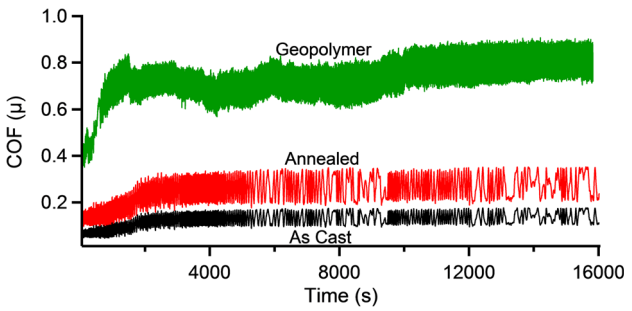

Fig. 4 Comparison of coefficient of friction plotted against time

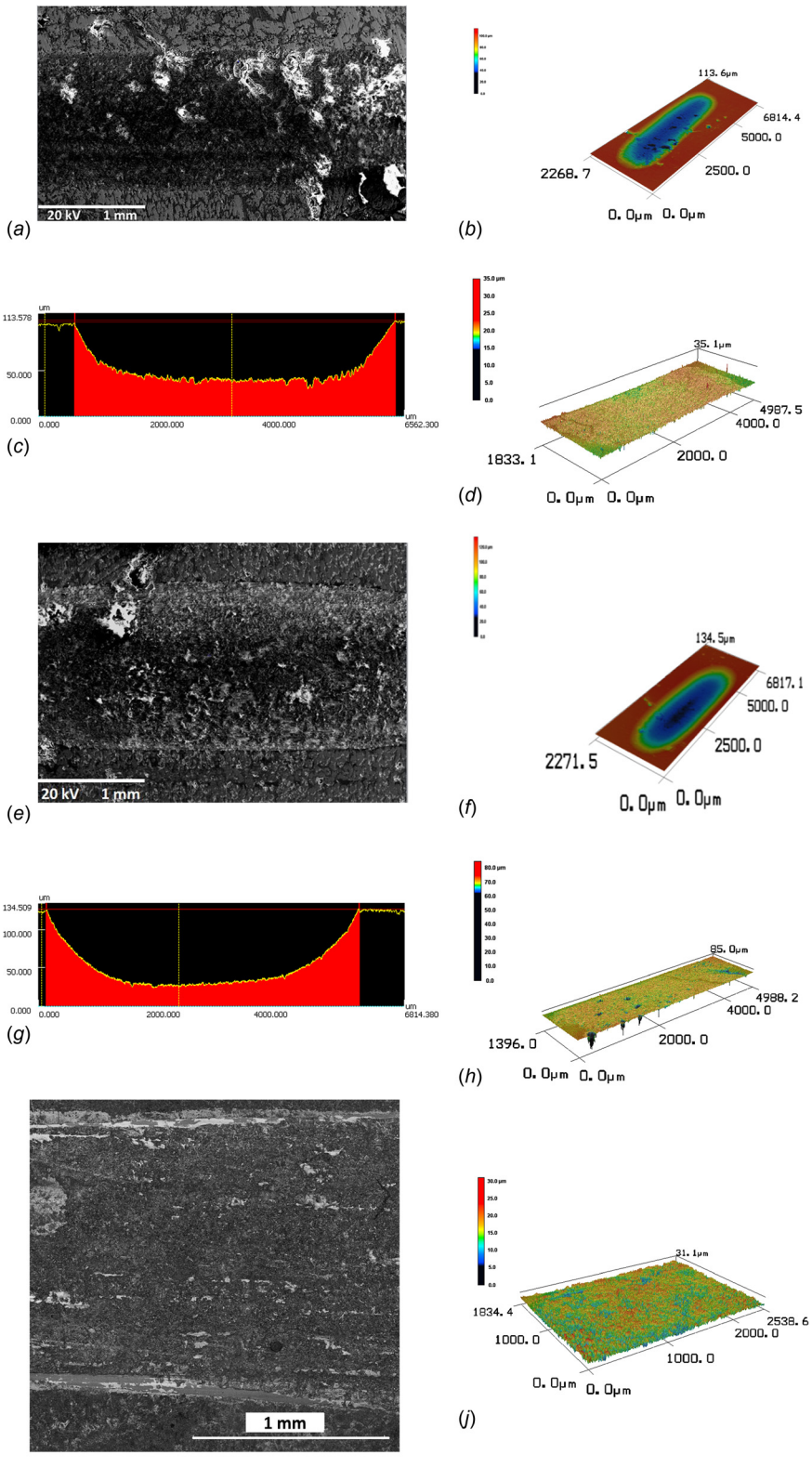

Fig. 5 (*a*) SEM image of as-cast $Al_{75}Mn_{14}Si_7Fe_4$, (*b*) 3D laser confocal microscopic surface height image of as-cast $Al_{75}Mn_{14}Si_7Fe_4$, (*c*) laser confocal microscopic two-dimensional image of as-cast $Al_{75}Mn_{14}Si_7Fe_4$ wear track, (*d*) 3D image of surface roughness profile of as-cast $Al_{75}Mn_{14}Si_7Fe_4$, (*e*) SEM image of annealed $Al_{75}Mn_{14}Si_7Fe_4$, (*f*) 3D laser confocal microscopic surface height image of annealed $Al_{75}Mn_{14}Si_7Fe_4$, (*g*) laser confocal microscopic two-dimensional image of annealed $Al_{75}Mn_{14}Si_7Fe_4$ wear track, (*h*) 3D image of surface roughness profile of annealed $Al_{75}Mn_{14}Si_7Fe_4$, (*i*) laser optical microscopic image of geopolymer, and (*j*) 3D image of surface roughness profile of geopolymer

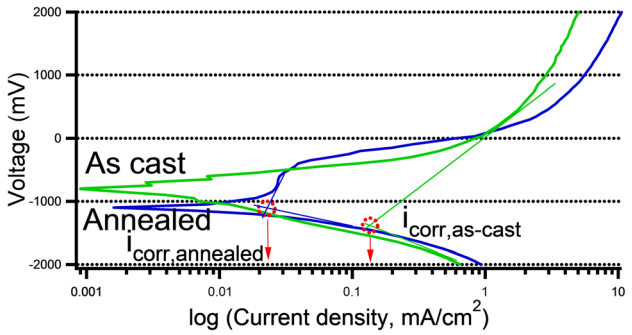

Fig. 6 Polarization curves of as-cast and annealed $Al_{75}Mn_{14}Si_7Fe_4$ alloy in 0.1 M NaCl solution

3.4 Corrosion Resistance. The polarization curves for the $Al_{75}Mn_{14}Si_7Fe_4$ alloys were obtained and shown in Fig. 6. Free corrosion potentials in 0.1 M NaCl solution were −800.1 mV for as-cast and −1100 mV for annealed condition. The current density of the annealed sample, $i_{corr,annealed}$, was almost an order magnitude lower than that of as-cast sample. However, although the current density was slightly higher and the oxide layer formation was earlier but it was followed by a quick destruction and a sharp increase in current density. Formation of a ferro-silico-alumina geopolymer phase may be the contributing factor toward the early formation of the oxide layer. Since the high strength icosahedral quasi-crystalline (*i*-phase) decreased from as-cast to annealed structure, it may be attributed as the reason for rapid destruction of this protective oxide layer against corrosion. The corrosion reaction for the quasi-crystalline $Al_{75}Mn_{14}Si_7Fe_4$ alloy in saline (0.1 M NaCl) solution can be formulated as follows:

$$3AlMnSiFe + 5NaCl + 3H_2O \rightarrow AlCl_3 + FeCl_2 + Al_2O_3 + 3H_2$$

$$Al \rightarrow Al^{3+} + 3e^-$$

$$1/2\ O_2 + H_2O + 2e^- \rightarrow 2OH^-$$

$$Al^{3+} + {}^{3OH-} \rightarrow Al(OH)_3$$

4 Conclusion

A quasi-crystalline $Al_{75}Mn_{14}Si_7Fe_4$-geopolymer composite with icosahedral phase was developed. The role of ferro-silico-alumina geopolymer phase on the wear and corrosion behavior of $Al_{75}Mn_{14}Si_7Fe_4$ quasi-crystalline alloy (with icosahedral structure) was studied. Microhardness showed the increase with existence of the icosahedral (*i*-phase) phase. The relative amount of icosahedral phase (about 70%) was attributed to the increased hardness and wear resistance. The geopolymer phase, on the other hand, is responsible for increased corrosion resistance. This study is beneficial for future design and development of composite materials targeting wear and corrosion resistance.

Acknowledgment

The authors wish to thank Dr. Naugle for allowing us to use his arc melter and Huaping Xiao, Mohammad Motaher Hossain, and James Chrisman for critical discussion. The authors also wish to acknowledge Dr. Miladin Radovic for tips for making a geopolymer sample. Partial support by the Turbomachinery Research Laboratory and the Strategic Initiatives at the Texas A&M University is greatly appreciated.

References

[1] Shechtman, D., Schaefer, R. J., and Biancaniello, F. S., 1984, "Precipitation in Rapidly Solidified Al-Mn Alloys," Metall. Trans. A, **15**(11), pp. 1987–1997.
[2] Dubois, J.-M., 2012, "Properties and Applications of Quasicrystals and Complex Metallic Alloys," Chem. Soc. Rev., **41**(20), pp. 6760–6777.
[3] Donnadieu, P., Lapasset, G., and Sanders, T. H., 1994, "Manganese-Induced Ordering in the Alpha-(Al-Mn-Fe-Si) Approximant Phase," Philos. Mag. Lett., **70**(5), pp. 319–326.
[4] Inoue, A., 1992, *Formation and High Mechanical Strength of Al-Based Alloys Containing a Nanoscale Icosahedral Phase as a Main Constituent*, Akita University, Institute for Materials Research, Akita, Japan, pp. 138–160.
[5] Bokhonov, B. B., 2008, "Mechanical Alloying and Self-Propagating High-Temperature Synthesis of Stable Icosahedral Quasicrystals," J. Alloys Compd., **461**(1–2), pp. 150–153.
[6] Barua, P., Srinivas, V., and Murty, B. S., 2000, "Synthesis of Quasicrystalline Phase by Mechanical Alloying of Al70Cu20Fe10," Philos. Mag. A, **80**(5), pp. 1207–1217.
[7] Shamah, A. M., Ibrahim, S., and Hanna, F. F., 2011, "Formation of Nano Quasicrystalline and Crystalline Phases by Mechanical Alloying," J. Alloys Compd., **509**(5), pp. 2198–2202.
[8] Huttunen-Saarivirta, E., 2004, "Microstructure, Fabrication and Properties of Quasicrystalline Al-Cu-Fe Alloys: A Review," J. Alloys Compd., **363**(1–2), pp. 150–174.
[9] Liu, W., Zhang, S., and Wang, L., 2012, "Ti1.4V0.6Ni Quasicrystal and Its Composites With xV(18)Ti(15)Zr(18)Ni(29)Cr(5)Co(7)Mn Alloy Used as Negative Electrode Materials for the Nickel-Metal Hydride (Ni-MH) Secondary Batteries," Mater. Lett., **79**, pp. 122–124.
[10] Kang, H., Li, X., Wang, T., Liu, D., Su, Y., Hu, Z., Guo, J., and Fu, H., 2014, "Crystal-Quasicrystal Transition Depending on Cooling Rates in Directionally Solidified Al-3Mn-7Be (at.%) Alloy," Intermetallics, **44**, pp. 101–105.
[11] Grushko, B., and Velikanova, T., 2007, "Formation of Quasiperiodic and Related Periodic Intermetallics in Alloy Systems of Aluminum With Transition Metals," Calphad, **31**(2), pp. 217–232.
[12] Koster, U., Liu, W., Liebertz, H., and Michel, M., 1993, "Mechanical-Properties of Quasi-Crystalline and Crystalline Phases in Al-Cu-Fe Alloys," J. Non-Cryst. Solids, **153**, pp. 446–452.
[13] Bendersky, L. A., Cahn, J. W., and Gratias, D., 1989, "A Crystalline Aggregate With Icosahedral Symmetry-Implication for the Crystallography of Twinning and Grain-Boundaries," Philos. Mag. B, **60**(6), pp. 837–854.
[14] Yan, Y. F., Wang, R. H., and Gui, J. I., 1990, "Stable and Metastable Phases in Some Quaternary Al-Si-Mn-Fe Alloys," J. Phys.: Condens. Matter, **2**(38), pp. 7733–7741.
[15] Dubois, J. M., and Lifshitz, R., 2011, "Quasicrystals: Diversity and Complexity," Philos. Mag., **91**(19–21), pp. 2971–2982.
[16] Dubois, J.-M., 1994, "Towards Applications of Quasicrystals," Mater. Sci. Eng., **A179/A180**, pp. 122–126.
[17] Bendersky, L. A., and Schaefer, R. J., 1986, "Formation of Quasi-Crystals," Phys. A, **140**(1–2), pp. 298–305.
[18] Mihoc, C., Nicula, R., Stir, M., Otterstein, E., and Burkel, E., 2012, *Synthesis of Quasicrystal/Polymer Composites*, Marie Curie Fellowship Association, Germany.
[19] Anderson, B. C., Bloom, P. D., Baikerikar, K. G., Sheares, V. V., and Mallapragada, S. K., 2002, "At-Cu-Fe Quasicrystal/Ultra-High Molecular Weight Polyethylene Composites as Biomaterials for Acetabular Cup Prosthetics," Biomaterials, **23**(8), pp. 1761–1768.
[20] Bloom, P. D., Baikerikar, K. G., Anderegg, J. W., and Sheares, V. V., 2003, "Fabrication and Wear Resistance of Al-Cu-Fe Quasicrystal-Epoxy Composite Materials," Mater. Sci. Eng. A, **360**(1–2), pp. 46–57.
[21] Bloom, P. D., Baikerikar, K. G., Otaigbe, J. U., and Sheares, V. V., 2000, "Development of Novel Polymer/Quasicrystal Composite Materials," Mater. Sci. Eng. A, **294–296**, pp. 156–159.
[22] Bloom, P. D., Baikerikar, K. G., Anderson, B. C., Mallapragada, S. K., and Sheares, V. V., 2001, "Ultra High Molecular Weight Polyethylene Quasicrystal Composites for Hip Arthroplasty Femoral Components," Abstr. Pap. Am. Chem. Soc., **222**, p. U394.
[23] Bloom, P. D., Baikerikar, K. G., and Sheares, V. V., 2000, "Wear Properties of Novel Al-Cu-Fe Quasicrystal-Polymer Composites," Abstr. Pap. Am. Chem. Soc., **219**, p. U489.
[24] Liu, Y. J., Bloom, P. D., Sheares, V. V., and Otaigbe, J. U., 2002, "A Novel Polyamide 12/Al-Cu-Fe Quasicrystal Composite," *Advanced Fibers, Plastics, Laminates and Composites*, F. T. Wallenberger, N. E. Weston, R. Ford, R. P. Wool, and K. Chawla, eds., Materials Research Society, Boston, MA, pp. 339–344.
[25] Huttunen-Saarivirta, E., and Tiainen, T., 2004, "Corrosion Behaviour of Al-Cu-Fe Alloys Containing a Quasicrystalline Phase," Mater. Chem. Phys., **85**(2–3), pp. 383–395.
[26] Wang, X. L., Li, X. S., Zhang, Z. J., Zhang, S. S., Liu, W. Q., and Wang, L. M., 2011, "Preparation and Wear Resistance of Ti-Zr-Ni Quasicrystal and Polyamide Composite Materials," Philos. Mag., **91**(19–21), pp. 2929–2936.
[27] Duxson, P., Provis, J. L., Lukey, G. C., and Van Deventer, J. S. J., 2007, "The Role of Inorganic Polymer Technology in the Development of 'Green Concrete'," Cem. Concr. Res., **37**(12), pp. 1590–1597.
[28] Duxson, P., Mallicoat, S. W., Lukey, G. C., Kriven, W. M., and van Deventer, J. S. J., 2007, "The Effect of Alkali and Si/Al Ratio on the Development of Mechanical Properties of Metakaolin-Based Geopolymers," Colloids Surf., A, **292**(1), pp. 8–20.
[29] Davidovits, J., 1991, "Geopolymers-Inorganic Polymeric New Materials," J. Therm. Anal., **37**(8), pp. 1633–1656.
[30] Duxson, P., Fernandez-Jimenez, A., Provis, J. L., Lukey, G. C., Palomo, A., and van Deventer, J. S. J., 2007, "Geopolymer Technology: The Current State of the Art," J. Mater. Sci., **42**(9), pp. 2917–2933.
[31] Davidovits, J., 2008, "Physical Properties of Condensed Geopolymers," *Geopolymer Chemistry and Applications*, Materials Research Society, Boston, MA, pp. 335–351.

[32] Duxson, P., Lukey, G. C., and van Deventer, J. S. J., 2007, "Physical Evolution of Na-Geopolymer Derived From Metakaolin up to 1000 Degrees C," J. Mater. Sci., **42**(9), pp. 3044–3054.
[33] Davidovits, J., 1989, "Geopolymers and Geopolymeric Materials," J. Therm. Anal., **35**(2), pp. 429–441.
[34] Davidovits, J., and Davidovics, M., 1991, "Geopolymer-Ultra-High Temperature Tooling Material for the Manufacture of Advanced Composites," Geopolymer Tooling Material, **2**, pp. 1939–1949.
[35] Belena, I., Tendero, M. J. L., Tamayo, E. M., and Vie, D., 2004, "Study and Optimizing of the Reaction Parametres for Geopolymeric Material Manufacture," Bol. Soc. Esp. Cerám. Vidrio, **43**(2), pp. 569–572.
[36] Lecomte, I., Liegeois, M., Rulmont, A., Cloots, R., and Maseri, F., 2003, "Synthesis and Characterization of New Inorganic Polymeric Composites Based on Kaolin or White Clay and on Ground-Granulated Blast Furnace Slag," J. Mater. Res., **18**(11), pp. 2571–2579.
[37] Altidis, J. D., de Barros, S., de Souza, J., Torres, S. M., and De Lima, S. J. G., 2012, "Adhesion Tests in Quasicrystal Powders Reinforced Geopolymer Composites," *Advanced Powder Technology Viii, Pts 1 and 2*, L. Salgado, and F. Ambrozio, eds., Materials Research Society, Boston, MA, pp. 186–189.
[38] Altidis, J. D., Lima, S. J. G., Torres, S. M., Lima, B., Medeiros, E. S., and de Barros, S., 2014, "The Influence of Alloying Elements on Adhesive Properties of Epoxy-Quasicrystal Composites," J. Adhes., **90**(1), pp. 41–49.
[39] Ramesh, C. S., Pramod, S., and Keshavamurthy, R., 2011, "A Study on Microstructure and Mechanical Properties of Al 6061–TiB2 In-Situ Composites," Mater. Sci. Eng., A, **528**(12), pp. 4125–4132.
[40] Swaddiwudhipong, S., Zeng, K., Tho, K. K., and Liu, Z. S., 2005, "Simulation of Instrumented Indentation and Material Characterization," Mater. Sci. Eng., A, **390**(1–2), pp. 202–209.